

# Comparison of Secondary Doping and Thermal Treatment in Poly(diphenylamine) and Polyaniline Monitored by Resonance Raman Spectroscopy

G. M. do Nascimento, J. E. Pereira da Silva, S. I. Córdoba de Torresi, and M. L. A. Temperini\*

Departamento de Química Fundamental, Instituto de Química, Universidade de São Paulo, CP 26.077, CEP 05513-970, São Paulo, SP, Brazil

Received May 29, 2001

**ABSTRACT:** Changes in poly(diphenylamine) chains primarily doped with camphorsulfonic acid (PDPA-CSA) during the secondary doping process were spectroscopically characterized. The UV–vis–NIR spectrum of PDPA-CSA treated with *m*-cresol showed the NIR (1100 nm) tail of the band due to free-carrier absorption, confirming the increase of polymer conductivity. Resonance Raman and ESR results showed that, during this treatment, there was a conversion of diphenosemiquinone segments into diphenoquinoid ones. These results indicated that spinless species are the free carriers in this kind of polymer, which are in contrast with those observed for PANI-CSA treated with *m*-cresol. The thermal behavior of PDPA-CSA was also studied by in-situ resonance Raman and ESR spectroscopies. These results also indicated a conversion of diphenosemiquinone segments into diphenoquinoid ones. New bands in Raman spectra at high temperature presented by PANI and PDPA were assigned to oxidized structures having oxazine-like rings.

## Introduction

The processability of conducting polymers is the main problem when considering their technological applications. To circumvent this problem, several treatments have been used such as polymer heating, incorporation of substituents in the polymeric chain, or change in the nature of the dopant.<sup>1</sup> The replacement of inorganic acids, traditionally used in the doping process of polyaniline, by functionalized organic acids makes the polymer soluble in a series of organic solvents and enables the manufacture of conducting polymeric blends.<sup>2</sup>

The additional increase in polyaniline (PANI) conductivity due to the interaction of a functionalized organic acid dopant with an appropriate solvent was reported in the literature.<sup>2</sup> The authors associated the conductivity increase with a conformational change of the polymeric chain from a coil structure to a more extended one. The same phenomenon was also studied by Mac Diarmid et al.,<sup>3</sup> who introduced the term “secondary doping” to characterize the effect of certain solvents on PANI, “primarily doped” by a functionalized organic acid. The increase in conductivity is dependent on the solvent–dopant combination. The highest conductivity was found in the system formed by PANI, camphorsulfonic acid (CSA), and *m*-cresol.<sup>3</sup> The behavior of the system PANI-CSA–*m*-cresol was also investigated by Ikkala et al.,<sup>4,5</sup> who postulated a very particular arrangement of the PANI-CSA and *m*-cresol, evidencing the formation of a supramolecular complex.

However, several questions still need to be addressed, including, for example, the extension of the secondary doping effect to other polymers with chains different than PANI, such as poly(diphenylamine) (PDPA).

Recent results have shown that resonance Raman spectroscopy is a very useful tool for monitoring the secondary doping process of PANI-CSA and demonstrate that there is also a conversion of quinone segments into semiquinone ones. These results were cor-

roborated by electron spin resonance (ESR) measurements.<sup>6,7</sup>

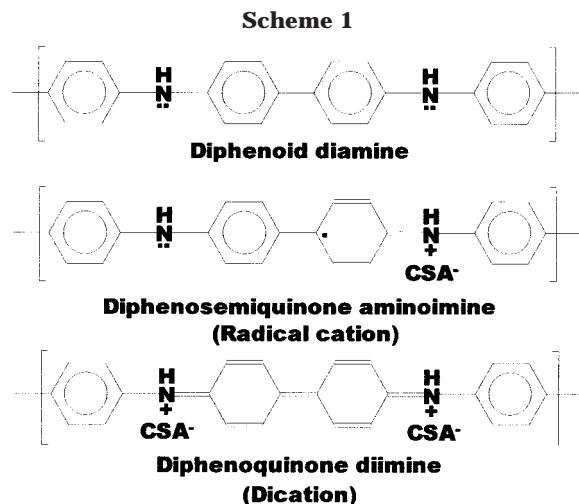
It is well-known that temperature is a very important parameter in the processability of conducting polymers, making important to understand the effect of thermal treatment on the oxidation state and structure of the polymeric chains.<sup>8</sup> It has been demonstrated that structural changes produced by thermal treatment in primarily and secondarily doped PANI-CSA are different in magnitude, but both polymers exhibit a decrease in quinone segments in the polymeric matrix. It was proposed that the increase in the temperature causes cross-linking and degradation (reaction with oxygen) of the polymeric matrix.<sup>7,9</sup>

The aim of this work was to verify the secondary doping in PDPA and to monitor the structural changes produced by heating the primarily doped polymers via resonance Raman, ESR, and UV–vis–NIR spectroscopies. These results are compared with those already obtained for PANI.

## Experimental Section

PDPA films doped with CSA were electrochemically grown (by potential sweeps between  $-0.2$  and  $+1.5$  V at a  $0.1$  V  $s^{-1}$  sweep rate) onto a platinum electrode in  $0.1$  M diphenylamine +  $0.2$  M CSA electrolytic solution with ethanol as solvent. A platinum wire was used as counter electrode, and all potentials were referred to the saturated calomel electrode (SCE). The same electrochemical procedure was used to grow PANI-CSA films. The potential range was  $-0.2$  to  $+0.75$  V, the sweep rate was  $0.05$  V  $s^{-1}$ , and the electrolytic solution was  $0.5$  M aniline +  $1$  M CSA aqueous solution.

Polymer films were grated from the electrode after drying, and the powders thus obtained were dissolved in *m*-cresol or in  $CHCl_3$  ( $6.2$  mg  $mL^{-1}$ ). The mixtures were treated in an ultrasonic bath until a substantial solubility had been achieved, as indicated by the color and viscosity of the polymer solution (typically from 4 to 10 h). The resulting solution was then filtered in order to obtain a limpid solution. Two ways were used for eliminating the *m*-cresol: by heating in air or by



heating in a vacuum. In the last case the secondary doped samples were sealed.

Resonance Raman spectra for 632.8 nm exciting radiation (He–Ne laser, Spectra Physics, model 127) and 457.9, 488.0, and 514.5 nm exciting radiation (Ar<sup>+</sup> laser, Omnichrome model 543-AP) were recorded with a Renishaw Raman imaging microscope (system 3000) containing an Olympus metallurgical microscope and a CCD detector. The laser beam was focused on the sample in a ca. 1  $\mu\text{m}$  spot by a  $\times 80$  lens. The laser power was always kept below 0.7 mW at the sample to avoid its degradation. FT-Raman spectra were recorded in a Bruker IFS66 optical system with an FRA 106 Raman module attachment with 1064 nm radiation from a Nd:YAG laser.

The Raman spectra as a function of temperature were obtained with a controlled temperature cell at a heating rate of 10  $^{\circ}\text{C min}^{-1}$  from room temperature to 150  $^{\circ}\text{C}$ . A TMS 92 (Linkam Scientific Instruments) temperature control module was used.

Thermogravimetric analyses were performed in a Hi-Res TGA 2950 (T.A. Inst.), using platinum crucibles with ca. 2 mg of the sample, under a nitrogen atmosphere at a heating rate of 20  $^{\circ}\text{C min}^{-1}$ .

ESR spectra were recorded from powders on a Bruker ER 200 spectrometer operating in the X-band ( $\sim 9.5$  GHz). Samples were extensively pumped out prior to investigation in order to eliminate *m*-cresol (secondarily doped samples) and ethanol or water (primarily doped samples).

UV–vis–NIR spectra of the polymers in solution were obtained in a Hitachi (model H100) spectrophotometer.

Resistivity measurements of polymer powders were performed by the two-point method using an Autolab PGSTAT30 impedance analyzer (Ecochemie) with FRA module. A dc potential of 0.0 V with a modulation of 5 mV (rms) was imposed in the 10 kHz to 10 mHz frequency range.

## Results and Discussion

The goal of this study is to verify the effect of secondary doping and thermal treatment on PDPA-CSA chains. This polymer contains the segments diphenoid diamine, diphenosemiquinone aminoimine (radical cation), and diphenokinone diimine (dication) (see Scheme 1) whose ratio in the polymeric matrix depends on its oxidation state.

Figure 1 shows the UV–vis–NIR spectrum of PDPA-CSA in  $\text{CHCl}_3$  (Figure 1A) which can be compared with that of PDPA-CSA in *m*-cresol (Figure 1B). As can be seen, there is an increase in the absorption in the near-infrared region only in the spectrum of PDPA-CSA in *m*-cresol; this increased absorption is the tail of the free carrier band formed during the treatment of PDPA-CSA with *m*-cresol.<sup>2</sup> These results show that secondary

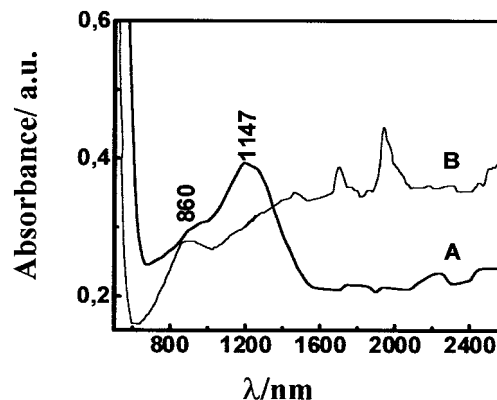


**Figure 1.** Electronic UV–vis–NIR absorption spectra of PDPA-CSA solutions: (A) in  $\text{CHCl}_3$  and (B) in *m*-cresol.

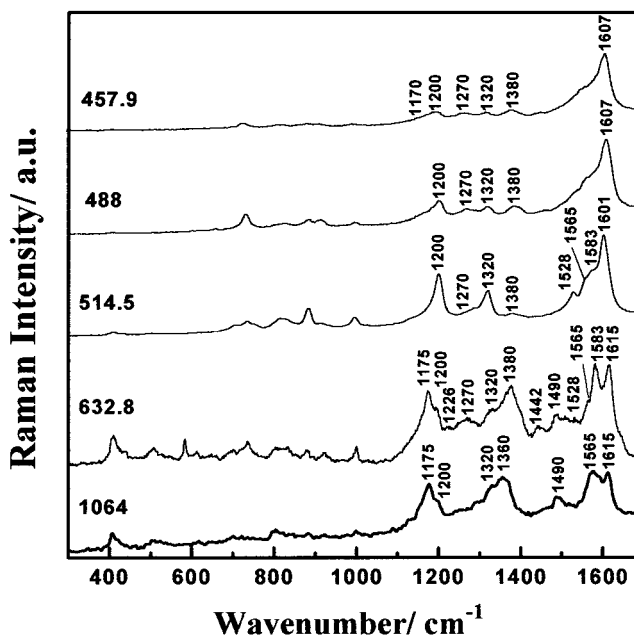


**Figure 2.** Resonance Raman spectra of primarily doped PDPA-CSA with several exciting radiations.

doping also occurs in conducting polymers with a backbone chain different from that of PANI.

The ac conductivity measurements of primarily and secondarily doped PDPA-CSA showed a ca. 20-fold increase, changing from  $4.2 \times 10^{-5} \text{ S cm}^{-1}$  for primarily doped polymer to  $7.6 \times 10^{-4} \text{ S cm}^{-1}$  for the polymer treated with *m*-cresol, providing additional evidence for the secondary doping of this polymer.

To monitor changes in the polymeric matrix during secondary doping process, the characteristic Raman bands of the primarily doped PDPA-CSA must be correlated with the structures. So the resonance Raman spectra of primarily doped PDPA-CSA were obtained with several excitation lines (Figure 2). As can be seen, there are significant changes in the relative intensities of the bands with the excitation wavelength. Using previous spectroscopic studies of PDPA, in which assignments of the bands and the resonance Raman condition for each structures were presented,<sup>10,11</sup> the bands at 1175 ( $\beta\text{C-H}$ , deformation in-plane), 1380 ( $\nu\text{C-C}$ , inter-ring stretching), 1490 ( $\nu\text{C-N}$ ), and 1583  $\text{cm}^{-1}$  ( $\nu\text{C-C}$ , ring stretching) can be assigned to dication segments since they have the highest relative intensities when the excitation radiation is 632.8 or 1064 nm. For 514.5 nm radiation, the relative intensities of the bands

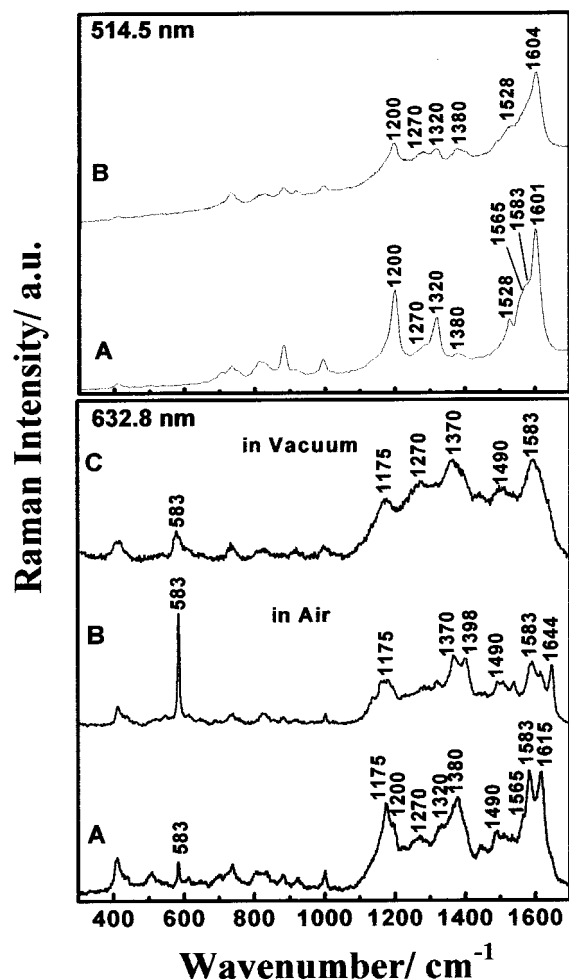


**Figure 3.** Resonance Raman spectra at  $\lambda_0 = 514.5$  and  $632.8$  nm of (A) primarily doped PDPA-CSA and secondarily doped PDPA-CSA obtained after (B) eliminating *m*-cresol by heating in air or (C) heating in a vacuum and the sample sealed.

at  $1200$  ( $\beta$ C–H),  $1320$  ( $\nu$ C–C inter-ring), and  $1565$   $\text{cm}^{-1}$  ( $\nu$ C–C ring) increase and can be attributed to the radical cation segments. For  $457.9$  nm, the most intense band at  $1607$   $\text{cm}^{-1}$  ( $\nu$ C–C ring) can be assigned to diphenoid diamine structures.

Figure 3 shows the Raman spectra of primarily and secondarily doped PDPA-CSA obtained with  $514.5$  and  $632.8$  nm excitation lines. For the green line, the relative intensities of the radical cation bands at  $1200$ ,  $1320$ , and  $1571$   $\text{cm}^{-1}$  decrease in the spectrum of the secondarily doped polymer, while the band at  $1380$   $\text{cm}^{-1}$ , due to dication, increases. The same behavior is observed using the  $632.8$  nm excitation line; the Raman bands of the radical cation ( $1200$  and  $1320$   $\text{cm}^{-1}$ ) practically disappear in the spectra of the secondarily doped polymer (B and C), while the dication features at  $1175$ ,  $1380$ ,  $1490$ , and  $1583$   $\text{cm}^{-1}$  are the most prominent bands. These changes suggest the transformation of radical cation units into dication ones, in clear contrast with the behavior observed for PANI-CSA treated with *m*-cresol.<sup>7</sup>

Although both spectra B and C ( $\lambda_0 = 632.8$  nm) correspond to secondarily doped PDPA, they show different features that can be related to the different ways of eliminating *m*-cresol. The strong bands at  $583$ ,  $1398$ , and  $1644$   $\text{cm}^{-1}$  only appear in spectrum B, and they are hence clearly related to a structure formed as the result of heating the polymer in the presence of oxygen. This point will be discussed later.

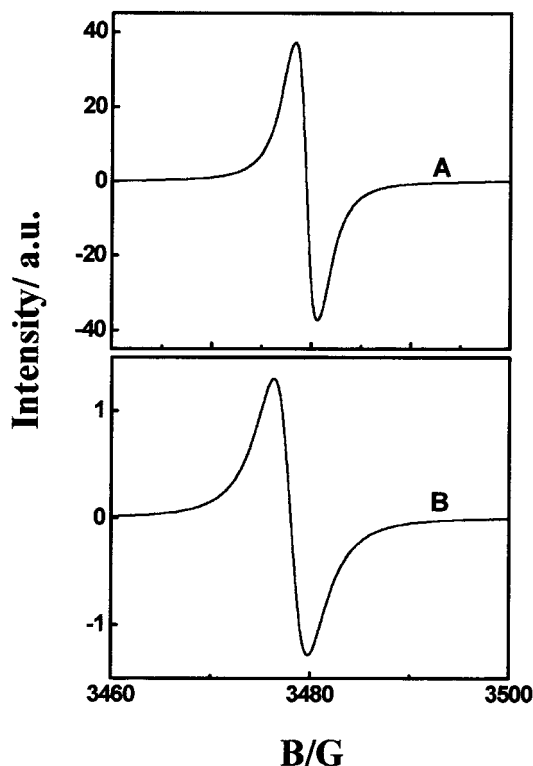


**Figure 4.** ESR spectra of polymer powders (A) primarily doped PDPA-CSA and (B) secondarily doped PDPA-CSA.

To confirm the resonance Raman results, ESR experiments were performed. Figure 4 shows the ESR spectra of PDPA-CSA powders obtained after solvent evaporation from the solutions prepared in  $\text{CHCl}_3$  (Figure 4a) and in *m*-cresol (Figure 4b). The integrated area in the primarily doped PDPA-CSA spectrum is 17 times greater than that calculated for the secondarily doped sample, indicating a decrease in the spin concentration after the treatment with *m*-cresol. These results corroborate those obtained by the resonance Raman technique, which shows a conversion of paramagnetic diphenosemi-quinoid segments into diamagnetic diphenquinoid units.

The results suggest that the dications are the main free carriers in the case of secondarily doped PDPA-CSA, while in the case of secondarily doped PANI-CSA, the radical cations are responsible for the near-infrared tail absorption.<sup>7</sup> Thus, a change in the polymeric backbone causes a transformation in the chemical nature of the free carriers in these two conducting polymers.

To monitor the influence of temperature on the nature of PDPA-CSA samples, in situ Raman spectra were obtained as a function of temperature. Before monitoring the changes provoked by heating the polymers, it was assured by TGA experiments that neither dedoping nor polymer decomposition occurs in the temperature range studied.

Figure 5 shows the Raman spectra as a function of temperature for primarily doped PDPA-CSA obtained with  $514.5$  and  $632.8$  nm excitation lines. For the green radiation, during heating in air, there is an increase in the relative intensities of the bands at  $1380$   $\text{cm}^{-1}$ , due to dication segments, and at  $1270$   $\text{cm}^{-1}$ , due to diphenyl diamine structures. Together with the appearance of these bands, there is a decrease in the relative intensity of the band located at  $1320$   $\text{cm}^{-1}$  due to the radical

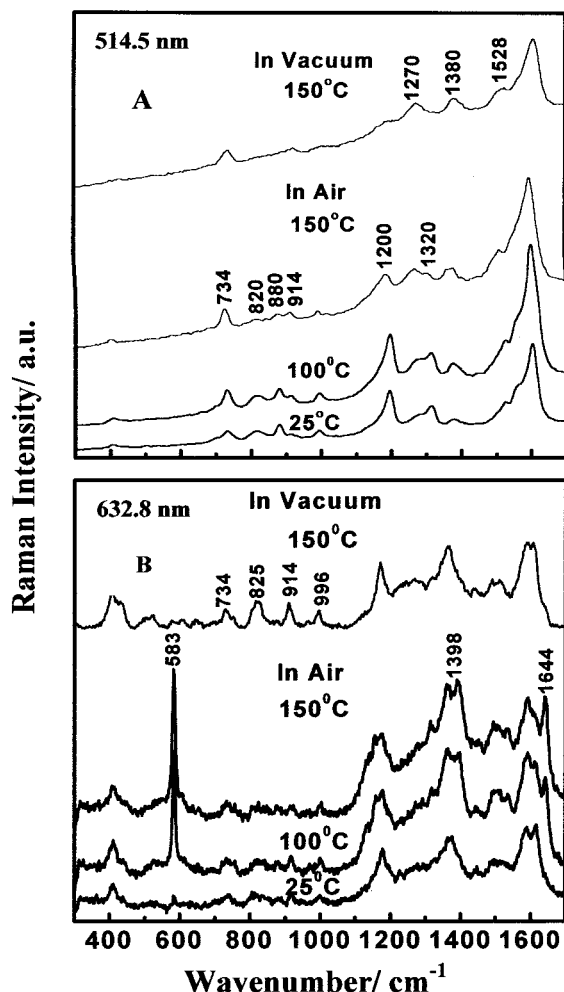


**Figure 5.** In situ resonance Raman spectra of primarily doped PDPA-CSA at different temperatures in an air atmosphere and preheated at 150 °C in a vacuum: (A) for 514.5 nm exciting radiation and (B) for 632.8 nm exciting radiation.

cation. This suggests that there is a conversion of radical cations into diphenylquinone diimine and diphenyl diamine segments with increasing temperature. This thermal conversion of segments is also observed when the polymer is heated in a vacuum up to 150 °C (top spectrum in Figure 5A). The same thermal conversion of segments has been observed for PDPA-BF<sub>4</sub> using FTIR<sup>11</sup> and was reported in poly(*p*-phenylenevinylene).<sup>12</sup>

Raman spectra obtained with the 632.8 nm line (Figure 5B) show that the PDPA-CSA powder undergoes significant changes during heating in air. At room temperature, the bands located at 583, 1398, and 1644 cm<sup>-1</sup> are not observed; with the increase of the temperature they start to grow and become some of the most intense bands in the spectrum at 150 °C. These bands are not observed in the Raman spectra of the polymer heated in air excited with 514.5 nm, indicating that these features are from some chromophoric structure that has a resonance Raman condition near 632.8 nm. It is important to note that these bands are not observed in the spectrum of the polymer sealed in a vacuum and heated to 150 °C (top spectrum in Figure 5B), suggesting that these features come from a structure produced by oxidation of the polymeric matrix. The Raman spectra of certain blue dyes with oxazine-type structures present very strong bands at ca. 580, 1380, and 1640 cm<sup>-1</sup>,

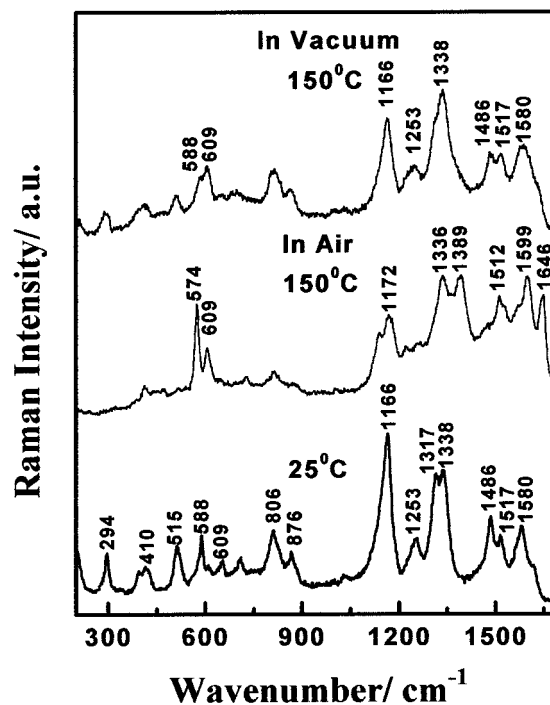


**Figure 6.** Resonance Raman spectra at  $\lambda_0 = 632.8$  nm of primarily doped PANI-CSA at room temperature in an air atmosphere and preheated at 150 °C in air and in a vacuum.

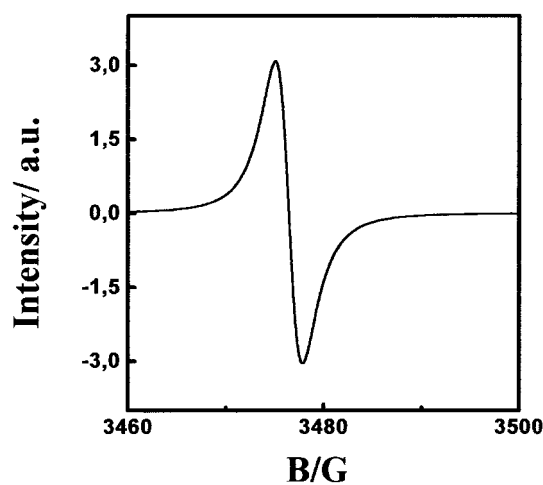


**Figure 7.** ESR spectrum of primarily doped PDPA-CSA powder preheated at 150 °C in air.

suggesting that these types of structures might be formed upon heating in air, resulting in a cross-linked network.

These bands have been observed in PANI-CSA spectra when heated in air;<sup>7</sup> for comparative purpose, Figure 6 shows the Raman spectra of PANI-CSA heated in both vacuum and air, confirming that the same or very similar chromophores are formed in the two polymers (PANI and PDPA).

Figure 7 shows the ESR spectrum of primarily doped PDPA-CSA powder preheated in air. Comparing this figure with Figure 4A, it can be seen that there is a significant decrease in the amount of paramagnetic units when the polymer is heated. As showed by Raman results, oxidation of the polymer due to oxygen and cross-linking occurs upon heating; the ESR results indicate that these structures are formed from paramagnetic centers.



## Conclusions

In this work it was shown that PDPA primarily doped with CSA can be secondarily doped when treated with *m*-cresol. The observation of the NIR tail of the absorption band attributed to the free carriers and the increase in the conductivity are evidences for the secondary doping effect. Resonance Raman spectroscopy shows that, during the secondary doping process, a conversion of diphenosemiquinone diamine (radical cation) units to diphenquinone diimine dication structures occurs. The decrease in the number of paramagnetic species in secondarily doped PDPA-CSA was confirmed by ESR spectroscopy. These results are strong evidence that the spinless species are favored during the secondary doping process. Comparing these results with those obtained for PANI-CSA, we can infer that dications species are the free carriers in the case of secondarily doped PDPA-CSA, while in the case of secondarily doped PANI-CSA, radical cations are responsible for the high conductivity.

New bands observed in the resonance Raman spectra, for 632.8 nm exciting radiation, of primarily doped PDPA-CSA and PANI-CSA powders heated in air are related to oxidized structures with oxazine-like rings that might be responsible for cross-linking.

**Acknowledgment.** This work was supported by FAPESP. Fellowships from FAPESP (G.M. do Nascimento and J.E.P. da Silva) and CNPq (S.I.C. de Torresi and M.L.A. Temperini) are gratefully acknowledged. Authors are also indebted to Profs. O. Augusto, A. M.

C. Ferreira, Y. Kawano, H. E. Toma, and M. Mancini for ESR, TG, and UV-vis-NIR facilities.

## References and Notes

- (1) Guay, J.; Leclerc, M.; Dao, L. H. *J. Electroanal. Chem.* **1988**, *251*, 31–39.
- (2) Cao, Y.; Smith, P.; Heeger, A. J. *Synth. Met.* **1992**, *48*, 91–97.
- (3) MacDiarmid, A. G.; Epstein, A. J. *Synth. Met.* **1994**, *65*, 103–116.
- (4) Ikkala, O. T.; Pietilä, L. O.; Ahjapalo, L.; Österholm, H.; Passiniemi, P. J. *J. Chem. Phys.* **1995**, *103*, 9855–9863.
- (5) Ikkala, O. T.; Pietilä, L. O.; Ahjapalo, L.; Österholm, H.; Passiniemi, P. J.; Vikki, T.; Österholm, J. E. *Synth. Met.* **1997**, *84*, 55–58.
- (6) Pereira da Silva, J. E.; Córdoba de Torresi, S. I.; Temperini, M. L. A. *Electrochim. Acta* **1999**, *44*, 1887–1891.
- (7) Pereira da Silva, J. E.; de Faria, D. L. A.; Córdoba de Torresi, S. I.; Temperini, M. L. A. *Macromolecules* **2000**, *33*, 3077–3083.
- (8) Boyle, A.; Penneau, J. F.; Geniès, E.; Riekel, C. *J. Polym. Sci., Part B* **1992**, *30*, 265–274.
- (9) Pereira da Silva, J. E.; Córdoba de Torresi, S. I.; de Faria, D. L. A.; Temperini, M. L. A. *Synth. Met.* **1999**, *101*, 834–835.
- (10) de Santana, H.; Temperini, M. L. A.; Rubim, J. C. *J. Electroanal. Chem.* **1993**, *356*, 145–155.
- (11) de Santana, H.; Matos, J. R.; Temperini, M. L. A. *Polym. J.* **1998**, *30*, 315–321.
- (12) Sakamoto, A.; Furukawa, Y.; Tasumi, M. *J. Phys. Chem.* **1992**, *96*, 3870–3874.
- (13) Wiedera, J.; Grachala, W.; Jackowska, K.; Bukowska, J. *Synth. Met.* **1997**, *89*, 29–37.
- (14) Yamada, H.; Nagata, H.; Kishibe, K. *J. Phys. Chem.* **1986**, *90*, 818–823.

MA010920H